Published in final edited form as:
Inorg Chem. 2004 April 5; 43(7): 2402–2415.

Proton Control of Oxidation and Spin State in a Series of Iron Tripodal Imidazole Complexes

Cynthia Brewer, **Greg Brewer***, **Charles Luckett**, and **Gwen S. Marbury**
Department of Chemistry, The Catholic University of America, Washington, D.C. 20064

Carol Viragh
Vitreous State Laboratory, The Catholic University of America, Washington, D.C. 20064

Alicia M. Beatty and **W. Robert Scheidt**
Department of Chemistry and Biochemistry, University of Notre Dame, Notre Dame, Indiana 46556

Abstract

Reaction of iron salts with three tripodal imidazole ligands, $H_3(1)$, $H_3(2)$, $H_3(3)$, formed from the condensation of tris(2-aminoethyl)amine (tren) with 3 equiv of an imidazole carboxaldehyde yielded eight new cationic iron(III) and iron(II), $[FeH_3L]^{3+or2+}$, and neutral iron(III), FeL, complexes. All complexes were characterized by EA(CHN), IR, UV, Mössbauer, mass spectral techniques and cyclic voltammetry. Structures of three of the complexes, Fe(2)·$3H_2O$ ($C_{18}H_{27}FeN_{10}O_3$, $a = b = c = 20.2707(5)$, cubic, $I\bar{4}3d$, $Z = 16$), Fe(3)·$4.5H_2O$ ($C_{18}H_{30}FeN_{10}O_{4.5}$, $a = 20.9986(10)$, $b = 11.7098(5)$, $c = 19.9405(9)$, $\beta = 109.141(1)$, monoclinic, $P2(1)/c$), $Z = 8$), and $[FeH_3(3)](ClO_4)_2 \cdot H_2O$ ($C_{18}H_{26}Cl_2FeN_{10}O_9$, $a = 9.4848(4)$, $b = 23.2354(9)$, $c = 12.2048(5)$, $\beta = 111.147(1)°$, monoclinic, $P2(1)/n$, $Z = 4$) were determined at 100 K. The structures are similar to one another and feature an octahedral iron with facial coordination of imidazoles and imine nitrogen atoms. The iron(III) complexes of the deprotonated ligands, Fe(1), Fe(2), and Fe(3), are low-spin while the protonated iron(III) cationic complexes, $[FeH_3(1)](ClO_4)_3$ and $[FeH_3(2)](ClO_4)_3$, are high-spin and spin-crossover, respectively. The iron(II) cationic complexes, $[FeH_3(1)]S_4O_6$, $[FeH_3(2)](ClO_4)_2$, $[FeH_3(3)](ClO_4)_2$, and $[FeH_3(3)][B(C_6H_5)_4]_2$ exhibit spin-crossover behavior. Cyclic voltammetric measurements on the series of complexes show that complete deprotonation of the ligands produces a negative shift in the Fe(III)/Fe(II) reduction potential of 981 mV on average. Deprotonation in air of either cationic iron(II) or iron(III) complexes, $[FeH_3L]^{3+or2+}$, yields the neutral iron(III) complex, FeL. The process is reversible for Fe(3), where protonation of Fe(3) yields $[FeH_3(3)]^{2+}$.

Introduction

The sensitivity of the Fe(III)/Fe(II) redox couple to the protonation level of coordinated imidazole ligands is important in view of synthetic interest in complexes of imidazole or imidazole-like ligands and in light of the special biological relevance of imidazole as a ligand in numerous heme proteins. For example, it has been known for some time that H-bonding to coordinated imidazole in an iron porphyrin significantly shifts the reduction potential for the Fe(III)/Fe(II) couple to favor the higher oxidation state.[1] Strong H-bonding of the proximal histidine has been suggested to account for the ease with which some peroxidases are oxidized, as compared to the oxygen carriers hemoglobin and myoglobin.[2] Moreover, deprotonation of

* To whom correspondence should be addressed. E-mail: brewer@cua.edu.

Supporting Information Available: Listings of crystal data, structure solution and refinement, atomic coordinates, bond lengths and angles, and anisotropic thermal parameters for complexes Fe(2)·$3H_2O$, Fe(3)·$4.5H_2O$, and $[FeH_3(3)](ClO_4)_2 \cdot H_2O$. This material is available free of charge via the Internet at http;//pubs.acs.org.

the proximal imidazole in several chelated heme model complexes results in immediate oxidization in air, even at low temperatures.[2]

Examples of proton-coupled electron transfer (PCET) or the coupling of proton transfer at a coordinated ligand with a metal-centered electron transfer are abundant among transition metal complexes.[3] PCET has been observed among aquo, hydroxo, oxo,[4–7] amine,[8–10] imidazole,[11,12] and other *N*-heterocyclic[13–15] and oxime[16–18] complexes of transition metal complexes, so it is not surprising that deprotonation of imidazole (or the less extreme case of strong H-bonding) should affect the reduction potential of a metal ion to which it is bound. In an extensive study of redox reactions of complexes of ruthenium and osmium containing benzimidazole subunits, Haga et al.[19,20] measured the effect of deprotonation of a coordinated benzimidazole ligand on the M(III)/M(II) reduction potential to be a shift of ~300 mV/proton in the negative direction. Williams et al.[21] have recently reported the structure and electrochemistry of an iron(II) complex of a 2,6-diimidazolyl pyridine, $[Fe(H_2(6))_2]^{2+}$ (see Figure 1). The potential for the Fe(III)/Fe(II)couple of $[Fe(H_2(6))_2]^{2+}$ is found at +0.920 mV vs NHE in acetonitrile. Upon deprotonation of the ligands in air (a loss of four protons), spontaneous oxidation is observed, and a new reduction potential is measured at −0.460 mV for $Fe(6)_2^-$, a negative shift of ~345 mV/proton. The reaction is not reversible on acidification. Reaction of Fe(III) with the protonated ligand in a 1:2 ratio does not result in isolation of $[Fe(H_2(6))_2]^{2+}$ or $[Fe(H_2(6))_2]^{3+}$, but instead, the 1:1 Fe(III) complex, $FeH_2(6)Cl_3$. Another PCET reaction involves an iron(II) tris complex of an α-diimine (N═C–C═N) ligand, 2,2′-bi-2-imidazoline, which undergoes oxidation in air to an iron(III) complex with spontaneous deprotonation of one of the coordinated ligands.[22] The electrochemical evidence suggests that for N_6 complexes containing imidazole, protonation of the imidazolate favors the iron(II) oxidation state, whereas the iron(III) oxidation state is stabilized with imidazolate, and that reaction of iron(II) complexes of imidazole with base in air can result in iron oxidation.

Presented here is the acid–base and redox chemistry of the iron(II) and iron(III) complexes of $H_3(L)$ (L = 1–3 depicted in Figure 1) and their corresponding anions, L^{3-} and their structural and electronic characterization. These ligands contain an encapsulating N_6 hexadentate donor set that ties up all coordination sites so that the metal/ligand stoichiometry cannot change during either redox or acid–base reactions and that can bind to both iron(II) and iron(III). They contain three imidazoles (~300mV/proton) to ensure that there is a significant difference (~1V) in reduction potentials between the imidazole (protonated) and imidazolate (deprotonated) forms. These complexes are also soluble in protic solvents, which facilitates study of acid–base chemistry. The iron(III) cationic complexes, $[FeH_3L]^{3+}$, produce iron(III) neutrals, FeL, in base, and the iron(II) cationic complexes, $[FeH_3L]^{2+}$, produce iron(III) neutrals, FeL, when reacted with base in air or with lead(IV) oxide and alumina. More importantly, on acidification in air, the iron(III) neutral complex, Fe(3), produces the iron(II) cationic complex, $[FeH_3(3)]^{2+}$. Thus, there is an acid–base-promoted reversible redox process.

$$Fe(3) + e^- \overset{H^+}{\rightarrow} [FeH_3(3)]^{2+}$$

Observations of oxidation of iron(II) under basic conditions and reduction of iron(III) under acidic conditions are presented with minimal mechanistic rationale at this time.

The protonation state of the ligands can also be expected to affect spin state selection for these iron(II) and iron(III) complexes. Spin state assignments were made from Mössbauer data obtained for the imidazole (protonated) and imidazolate (deprotonated) iron complexes reported here, and a correlation between the level of protonation and the observed spin state is presented.

Structures of Fe(2), Fe(3) and $[FeH_3(3)](ClO_4)_2$ are reported here whereas that of Fe(1) was the result of earlier work in this laboratory.[23] Other iron structures of these ligands include an adduct of Fe(3) and $Mn(hfa)_2$,[24] an adduct of 4-imidazolecarboxaldehyde and $[FeH_3(2)](ClO_4)_3$,[25] and a 2D mixed-valence polymer, $[FeH_3(2)][Fe(3)](NO_3)_2$.[26] Structures of the closely related complexes (ligands depicted in Figure 1) $[Fe(4)](PF_6)_2$[27] and $[Fe(5)](BF_4)_2$[28] are also known. These last two species cannot undergo the deprotonation reactions of iron complexes of H_3(1–3); however, they are mentioned here due to their importance in understanding the redox chemistry of the iron complexes of H_3(1–3) and the spontaneous aerial reduction of iron(III) to iron(II) in the presence of H_3(3).

These observations have implications for biological redox systems, such as the oxygen-reducing enzymes, cytochrome *c* peroxidase and horseradish peroxidase,[29] and the oxygen-evolving system of Photosystem II.[30] Although the latter system contains a polynuclear manganese core and the present complexes are mononuclear iron, it is mentioned here because it involves a metal redox change coupled to dioxygen chemistry.

Experimental Section

Elemental analyses were determined by MHW Laboratory, Phoenix, AZ. Mass spectral analyses were obtained from HT Laboratories, San Diego, CA, or the Mass Spectrometry Center, UMass, Amherst, MA. Tris(2-aminoethyl)amine, 4-methyl-5-imidazole carboxaldehyde, 4-imidazole carboxaldehyde, 2-imidazole carboxaldehyde, anhydrous ferric chloride, sodium tetraphenylboron, triethylamine, standardized 0.1 M sodium hydroxide, aluminum oxide (neutral Brockmann I, 150 mesh), and silica gel (grade 62, 60–200 mesh) were obtained from Aldrich. Ferrous perchlorate hexahydrate was obtained from Alfa. Ferrous chloride tetrahydrate, sodium perchlorate monohydrate, and sodium thiosulfate pentahydrate were obtained from Fisher. Powdered lead dioxide was purchased from J. T. Baker. All solvents were of reagent grade and were used without further purification.

Spectra

The ^{57}Fe Mossbauer specta were recorded from powdered samples with a constant acceleration using a MS1200 Ranger Scientific spectrometer and a ~1.85 GBq ^{57}Co/Rh source. The sample thickness was 50–80 mg/cm^2. The line width of the calibration spectrum was 0.29 mm/s. The chemical isomer shift data are quoted relative to the centroid of the metallic iron spectrum at room temperature. The data were analyzed by a constrained least-squares fit to Lorentzian shaped lines. UV–visible spectra were obtained on a Perkin-Elmer Lambda 4 spectrometer. IR spectra were obtained as KBr pellets on a Perkin-Elmer 1600 FT IR spectrometer. ^{1}H NMR spectra were recorded on a JEOL 300-MHz pulsed FT NMR.

Structure Determinations

Crystalline samples were placed in inert oil, mounted on a glass fiber attached to a brass mounting pin, and transferred to the cold gas stream of the diffractometer. Crystal data were collected and integrated using a Bruker Apex system, with graphite–monochromated Mo K_α (λ = 0.710 73 A) radiation. Data collections were carried out at 100 K for all complexes. All structures were solved using the direct methods program SHELXS.[31] All nonsolvent heavy atoms were located using subsequent difference Fourier syntheses. The structures were refined against F^2 with the program SHELXL,[32] in which all data collected were used, including negative intensities. All nonsolvent heavy atoms were refined anisotropically. All nonsolvent hydrogen atoms were idealized using the standard SHELXL idealization methods. Complete crystallographic details are given in the Supporting Information and are summarized in Table 1. In Fe(2)·3H_2O, one-third of the molecule is crystallographically unique, and the water molecule was disordered over two positions related by a 2-fold axis of symmetry. For Fe(3),

there are two independent molecules in the asymmetric unit of structure. In $FeH_3(3)](ClO_4)_2$, one of the perchlorate counterions is disordered over two positions.

Cyclic Voltammetry

Cyclic voltammograms were obtained under N_2 with a Bioanalytical Systems CV-27 cyclic voltammograph at a platinum electrode. Data were obtained in about 1 mM solutions of the iron complexes in acetonitrile using 0.1 M tetra-*n*-propylammonium perchlorate as the supporting electrolyte. The $E_{1/2}$ potentials are referenced to the silver/silver ion electrode.

Potentiometric Titrations

Potentiometric titrations were performed with a Denver Instruments Basic pH meter using a glass bodied pH/ATC combination electrode on the mV scale. Measurements were done in air at 23 °C. The solvent system, DMF/water (4:1), was chosen to facilitate solubility of both $[FeH_3(1)](ClO_4)_3$ and $[FeH_3(3)](BPh_4)_2$. Ionic strength was adjusted to 0.100 with sodium perchlorate. Standardized sodium hydroxide was used as the titrant (see Figures 2 and 3).

Syntheses. Caution!

Perchlorate salts of metal complexes with organic ligands are potentially explosive and should be handled with care.

H_3(1–3)

The free ligands can be prepared by the following general procedure; however, in the synthesis of the iron complexes which follow, the iron salt was added to a reaction mixture of tren and the appropriate imidazole carboxaldehyde without prior isolation of the ligand. A mixture of the imidazolecarboxaldehyde (4.00 mmol) and tren (195 mg, 1.33 mmol) in 40 mL methanol was refluxed for 60 min to give a yellow solution. The methanol was allowed to evaporate, and the resultant oil was stirred in ethyl acetate overnight. The resulting off-white solid was isolated by filtration.

H_3(1)—^{1}H NMR in DMSO-d_6 2.25 (s, 3H, CH_3), 2.78 (t, 2H, N–CH_2CH_2) 3.54 (t, 2H, N–CH_2CH_2), 7.53 (s, 1H, C_{Im}–H), 8.18 (s, 1H, N_{Imine}═CH). MS(ES pos, MeOH): *m*/*z* = 423 $(M + H)^+$. Yield: 69%.

H_3(2)—^{1}H NMR in DMSO-d_6 2.75 (t, 2H, N–CH_2CH_2) 3.52 (t, 2H, N–CH_2CH_2), 7.25 (s, 1H, C_{Im}–H). 7.69 (s, 1H, C_{Im}–H) 8.08 (s, 1H, N_{Imine}═CH). MS(ES pos, MeOH): *m*/*z* = 381 $(M + H)^+$. Yield: 26%.

H_3(3)—^{1}H NMR in DMSO-d_6 2.82 (t, 2H, N–CH_2CH_2) 3.61 (t, 2H, N–CH_2CH_2), 7.16 (s, 2H, C_{Im}–H), 8.16 (s, 1H, N_{Imine}═CH). MS(ES pos, MeOH): *m*/*z* = 381 $(M + H)^+$. Yield: 40%.

The exchangeable NH imidazole proton was not observed between 0 and 15 ppm under these conditions; however, evidence for the imidazole NH proton is found in the IR spectrum.

$[FeH_3(1)](ClO_4)_3$

Method a (from $FeCl_3$ and H_3(1))—A mixture of 4-methyl-5-imidazolecarboxaldehyde (425 mg, 3.86 mmol) and tren (195 mg, 1.33 mmol) in 40 mL of methanol was stirred and refluxed for 15–20 min to give a yellow solution. Anhydrous $FeCl_3$ (210 mg, 1.3 mmol) in 15 mL of methanol was added. The reaction mixture immediately turned purple. The reaction mixture was stirred and refluxed for 10 min. Sodium perchlorate monohydrate (1200 mg, 8.6 mmol) in 5–10 mL of methanol was added all at once to the reaction mixture. Within 10–15 min, small purple crystals of $[FeH_3(1)](ClO_4)_3$ had formed. After several hours, 831 mg of

small purple crystals were isolated by filtration. Yield: 84%. Elemental analysis calcd for $C_{21}H_{30}Cl_3N_{10}O_{12}Fe$: C 32.47, H 3.89, N 18.03. Found: C 32.72, H 4.19, N 17.83.

Method b (from Protonation of Fe(1))—Aqueous hydrochloric acid (0.100 M, 6.3 mL, 0.63 mmol) was added dropwise to a solution of Fe(1) (100 mg, 0.210 mmol) in methanol (40 mL) with stirring. The blue solution changed to green and, finally, purple during the addition. The solution was hot-filtered, and solid sodium perchlorate monohydrate (177 mg, 1.26 mmol) was added. The solution was taken to dryness, and the solid was recrystallized from methanol (80 mL). Hot filtration removed a small amount of brown solid. Concentration of this solution afforded 99 mg of purple solid, which was removed by filtration. Yield 60%.

$[FeH_3(1)]S_4O_6$

A slight excess of solid sodium thiosulfate pentahydrate (42 mg, 0.169 mmol) was added to a solution of $[FeH_3(1)](ClO_4)_3$ (100 mg, 0.129 mmol) in 60 mL of refluxing methanol. Within 5 min, the color changed from purple to pale orange, and the solution was filtered while hot to remove a small quantity of a red solid. Orange crystals began to form on cooling and were collected by filtration within a day. Yield: 30 mg, 33% based on iron. Elemental analysis calcd for $C_{23}H_{38}N_{10}S_4O_6Fe$ ($[FeH_3(1)]S_4O_6\cdot 2CH_3OH$): C 36.06, H 5.01, N 18.29. Found: C 36.45, H 4.88, N 18.45.

$[FeH_3(2)](ClO_4)_3$

A mixture of 4-imidazolecarboxaldehyde (403 mg, 4.19 mmol) and tren (205 mg, 1.40 mmol) in 25 mL of methanol was stirred and refluxed for 15–20 min to give a yellow solution. Anhydrous $FeCl_3$ (220 mg, 1.36 mmol) in 10–15 mL of methanol was added. The reaction mixture immediately turned dark red. The reaction mixture was stirred and refluxed for an additional 15–20 min. Sodium perchlorate monohydrate (1310 mg, 9.33 mmol) dissolved in 10 mL of methanol was added to the reaction mixture. Within 20 min, a red precipitate had begun to form. After several hours, the reaction mixture was filtered to remove 503 mg of a red powder. Yield: 47%. Elemental analysis calcd for $C_{18}H_{28}Cl_3N_{10}O_{14}Fe$ ($[FeH_3(2)](ClO_4)_3\cdot 2H_2O$): C 28.05, H 3.66, N 18.17. Found: C 28.13, H 3.48, N 18.40.

$[FeH_3(2)](ClO_4)_2$

A mixture of 4-imidazolecarboxaldehyde (385 mg, 4.01 mmol) and tren (195 mg, 1.33 mmol) in 30 mL of methanol was stirred and refluxed for 15 min to give a yellow solution. $Fe(ClO_4)_2\cdot 6H_2O$ (490 mg, 1.35 mmol) was added to the solution as a solid. The reaction mixture immediately turned red-orange. The reaction mixture was stirred and refluxed for an additional 5–10 min and then filtered while hot. The filtrate was allowed to concentrate. An orange precipitate began forming immediately. After several hours, 681 mg of orange crystals was removed by filtration. The product was recrystallized from ethanol to remove some brown solid. Final filtration gave 560 mg of small orange crystals. Yield: 61%. Elemental analysis calcd for $C_{19}H_{31}Cl_2N_{10}O_{10.5}Fe$ ($[FeH_3(2)](ClO_4)_2\cdot 2H_2O\cdot 0.5CH_3CH_2OH$): C 32.90, H 4.47, N 20.20. Found: C 32.63, H 3.98, N 19.98.

$[FeH_3(3)](ClO_4)_2$

Method a (from $FeCl_3$ and $H_3(3)$)—A mixture of 2-imidazolecarboxaldehyde (904 mg, 9.41 mmol) and tren (459 mg, 3.14 mmol) in 30 mL of methanol was stirred and refluxed for 30 min to give a pale yellow solution. Anhydrous $FeCl_3$ (510 mg, 3.1 mmol) in 10–15 mL of methanol was added. The reaction mixture immediately turned a deep blue, which persisted for less than 30 s, and then bright red. The reaction mixture was stirred and refluxed for 5–10 min and then removed from the heat source. Sodium perchlorate monohydrate (2000 mg, 14.3 mmol) dissolved in 10 mL of methanol was added. The solvent was removed from the reaction

mixture, and the residue was recrystallized from absolute ethanol to give 960 mg of red product. Yield: 49%. Elemental analysis calcd for $C_{18}H_{24}Cl_2N_{10}O_8Fe$: C 34.04, H 3.81, N 22.05. Found: C 34.41, H 4.17, N 22.12. A suitable crystal for X-ray structural determination was obtained by slow evaporation from an ethanol solution.

Method b (from $Fe(ClO_4)_2$ and $H_3(3)$)—A mixture of 2-imidazolecarboxaldehyde (388 mg, 4.04 mmol) and tren (195 mg, 1.33 mmol) in 25 mL of methanol was stirred and refluxed for 30 min to give a pale yellow solution. $Fe(ClO_4)_2 \cdot 6H_2O$ (510 mg, 1.4 mmol) was added as a solid. The reaction mixture immediately turned bright red. The reaction mixture was stirred and refluxed for 10 min and set aside to concentrate. The reaction mixture was taken nearly to dryness and the reddish solid that precipitated was recrystallized from absolute ethanol to give 509 mg of red product. Yield: 60%.

Method c (from Protonation of Fe(3))—Aqueous hydrochloric acid (0.100M, 1.73 mL, 0.17 mmol) was added dropwise to a solution of Fe(3) (25 mg, 0.058 mmol) in 20 mL of ethanol. The blue solution turned emerald green and was heated gently. Excess solid sodium perchlorate (32 mg, 0.23 mmol) was added to the green solution. On concentration, the green solution turned red and deposited a red solid that was slightly contaminated with a green-blue solid. The solids were slurried in acetone (10 mL) and applied to a silica column (0.5 × 1 in). A red band was eluted with acetone and collected. The column was then eluted with methanol to remove a very small blue band and leave a small amount of brown material at the top of the column. The red solution was taken to dryness, and the solid was recrystallized from ethanol (10 mL). Slow evaporation yielded 14 mg of red crystalline $[FeH_3(3)](ClO_4)_2$. Yield: 38%.

$[FeH_3(3)][B(C_6H_5)_4]_2$

Method a (from $FeCl_2$ and $H_3(3)$)—A mixture of 2-imidazolecarboxaldehyde (389 mg, 4.05 mmol) and tren (195 mg, 1.33 mmol) in 35 mL of methanol was stirred and refluxed for 15 min to give a pale yellow solution. $FeCl_2 \cdot 4H_2O$ (280 mg, 1.41 mmol) was added to the reaction mixture as a solid. The reaction mixture immediately turned red. It was stirred and refluxed for 5–10 min and filtered while hot. The filtrate was cooled to room temperature, and sodium tetraphenylborate (1820 mg, 5.33 mmol) dissolved in 20 mL of methanol was added. A total of 1148 mg of a red powder precipitated immediately. The product was recrystallized from 50:50 methanol/acetone. Yield: 80%. Elemental analysis calcd for $B_2C_{66}H_{64}N_{10}Fe$: C 73.76, H 6.00, N 13.03. Found: C 73.05, H 6.56, N 13.51.

Method b (from Protonation of Fe(3))—Aqueous hydrochloric acid (0.100 M, 1.7 mL, 0.173 mmol) was added dropwise to a solution of Fe(3) (25 mg, 0.058 mmol) in 20 mL of methanol. The blue solution turned to green upon addition of 20 drops of the acid. The green solution was gently warmed for a few minutes. Excess solid sodium tetraphenylborate (79 mg, 0.23 mmol) was added to the green solution, which caused a color change to violet. Within a minute, the solution was red, and a red precipitate had formed. The solution was filtered to remove 34 mg of red $[FeH_3(3)][B(C_6H_5)_4]_2$. Yield: 55%. The filtrate was pale blue and turned red and deposited more solid on addition of a few drops of acid. Elemental analysis calcd for $B_2C_{66}H_{64}N_{10}Fe$: C 73.76, H 6.00, N 13.03. Found: C 73.53, H 6.03, N 12.99.

Fe(1)

Method a (by Deprotonation of $[FeH_3(1)](ClO_4)_3$)—$[FeH_3(1)](ClO_4)_3$ (231 mg, 2.98 mmol) was dissolved in 10 mL of water. A 10.0-mL portion of 0.100 M NaOH was added dropwise with stirring. The color of the solution gradually changed from purple to blue, and 126 mg of blue Fe(1) precipitated. Yield: 89%.

Method b (by Oxidation of $[FeH_3(1)](S_4O_6$ with PbO_2)—Solid lead(IV) oxide (100 mg) was added in small portions to a slurry of $[FeH_3(1)]S_4O_6$ (50 mg, 0.071 mmol) in 20 mL of methanol. The orange solution changed to green within 5 min. The green solution was applied to a dry alumina column (0.5 × 6 in). On contact with the column the green solution turned blue. The blue band was eluted as a broad, unfocused band with methanol (40 mL), leaving the lead(IV) oxide on the column. This solution afforded 11 mg (32%) of Fe(1).

Method c (by Deprotonation of $[FeH_3(1)]S_4O_6$)—Aqueous sodium hydroxide (0.100 M, 2.1 mL, 0.21 mmol) was added dropwise to a slurry of $[FeH_3(1)](S_4O_6$ (50 mg, 0.071 mmol) in 20 mL of methanol. The color changed from orange to blue in 2 min. Concentration of this solution followed by filtration afforded 14 mg of Fe(1). Yield: 41%.

Fe(2)

Method a (by Deprotonation of $[FeH_3(2)](ClO_4)_3$ Generated "in Situ")—A solution of 4-imidazolecarboxaldehyde (400 mg, 4.16 mmol) and tren (195 mg, 1.33 mmol) in 30 mL of methanol was stirred and refluxed for 15 min. Anhydrous $FeCl_3$ (216 mg, 1.33 mmol) in 10 mL of methanol was added. The purple-red reaction mixture was stirred and refluxed an additional 5 min and then filtered while hot. To the filtrate was added 39.5 mL of aqueous sodium hydroxide (0.1010 M, 3.99 mmol), and the reaction mixture was stirred and refluxed for 10 min. The reaction mixture changed color from purplish red to deep blue. The reaction mixture was set aside to concentrate. A 397-mg portion of a blue microcrystalline solid was removed by filtration. The solid was recrystallized from a methanol/water mixture to give 308 mg of blue microcrystalline Fe(2). Yield: 45%. Elemental analysis calcd for $C_{20}H_{31}N_{10}O_3Fe$ (Fe(2)·$2CH_3OH·H_2O$): C 46.63, H 6.08, N 27.20. Found: C 46.40, H 5.66, N 27.12. A suitable crystal for X-ray structural determination was obtained by slow evaporation from a methanol–methylene chloride solution.

Method b (by Oxidation of $[FeH_3(2)](ClO_4)_2$ with PbO_2)—Solid lead(IV) oxide (100 mg) was added in small portions to a solution of $[FeH_3(2)](ClO_4)_2$ (50 mg, 0.079 mmol) in 20 mL of methanol. The orange solution changed to green within 5 min. The green solution was applied to a dry alumina column (0.5 × 6 in). On contact with the column, the green solution turned blue. The blue band was eluted as a broad, unfocused band with methanol (40 mL), leaving the lead(IV) oxide on the column. The methanol solution was taken to dryness, and the blue solid was applied to a dry silica column (0.5 × 3 in) and eluted with two column volumes of acetone to remove any soluble perchlorates. The blue complex was eluted in methanol (20 mL). This solution afforded 20 mg of Fe(2). Yield: 59%.

Fe(3)

Method a (by Deprotonation of $[FeH_3(3)]^{2+}$ Generated "in Situ")—A solution of 2-imidazolecarboxaldehyde (387 mg, 4.02 mmol) and tren (195 mg, 1.33 mmol) in 30 mL of methanol was stirred and refluxed for 20 min. $FeCl_2·4H_2O$ (266 mg, 1.34 mmol) was added as a solid. The reaction mixture immediately turned bright red. The mixture was stirred and refluxed for an additional 5–10 min. The reaction mixture, containing $[FeH_3(3)]^{2+}$, was filtered while hot, and the filtrate was cooled to room temperature. A 40-mL portion of aqueous sodium hydroxide (0.1010 M, 4.04 mmol) was added to the filtrate, and the solution was stirred 5–10 min. The reaction mixture changed color from bright red to deep blue. The solution was allowed to concentrate nearly to dryness. A blue-green solid was removed by filtration and recrystallized from a methanol–water mixture to give 491 mg of blue-green crystalline Fe(3). Yield: 85%. Elemental analysis calcd for $C_{18.5}H_{32}N_{10}O_{3.5}Fe$ (Fe(3)·$0.5CH_3OH·3H_2O$): C 44.15, H 5.81, N 27.83. Found: C 44.60, H 5.62, N 28.13 A suitable crystal for X-ray structural determination was obtained by slow evaporation from a methanol–methylene chloride solution.

Method b (by Oxidation of $[FeH_3(3)]X_2$ with PbO_2)—This method with slight modifications was used for X = perchlorate and tetraphenylborate. The modifications were needed due to the very different solubilities of the two salts and to ensure that the resultant product, Fe(3), was free of either starting material or simple salts of the anion. Both modifications are given.

X = ClO_4^-—Solid lead(IV) oxide (100 mg) was added in small portions to a solution of $[FeH_3(3)](ClO_4)_2$ (100 mg, 0.158 mmol) in 20 mL of methanol. The red solution changed to green within 2 min. The green solution was applied to a dry alumina column (0.5 × 6 in). On contact with the column, the green solution turned blue. The blue band was eluted as a broad, unfocused band with methanol, leaving the lead oxide on the column. This solution afforded 34 mg of Fe(3). Yield: 50%.

X = BPh_4^-—Solid lead(IV) oxide (100 mg) was added in small portions to a solution of $[FeH_3(3)](BPh_4)_2$ (100 mg, 0.0931 mmol) in 30 mL of acetone over a 2-h period. During this time, the red solution changed to green. The solution was applied to a dry alumina column (0.5 × 6 in). On contact with the column, the green solution turned blue. The blue band remained bound to the column, which was washed with two column volumes of acetone. The blue band was eluted as a tight band with 50/50 methanol/dichloromethane, leaving the lead oxide on the column. This solution was taken to dryness, and the resulting 32 mg of deep blue powder was recrystallized from methanol/water (20 mL:5 mL). On concentration, 18 mg of Fe(3) was removed by filtration. Yield: 45%.

Method c (by Deprotonation of $[FeH_3(3)]X_2$)—This method, with slight modifications, was used for X = perchlorate and tetraphenylborate. The modifications were needed due to the very different solubilities of the two salts and to ensure that the resultant product, Fe(3), was free of either starting material or simple salts of the anion. Both modifications are given.

X = ClO_4^-—Aqueous sodium hydroxide (0.100 M, 5.00 mL, 0.500 mmol) was added dropwise to a solution of $[FeH_3(3)](ClO_4)_2$ (100 mg, 0.157 mmol) in 20 mL of methanol. The solution changed in color from red to violet. An additional 2 mL of base was added and the solution was left to stand overnight during which time it changed the color to dark blue. Concentration of the aqueous methanol solution afforded 55 mg of Fe(3). Yield: 81%.

X = BPh_4^-—Triethylamine (TEA) (10 drops) was added dropwise to a solution of $[FeH_3(3)](BPh_4)_2$ (50 mg, 0.046 mmol) in 20 mL of acetone. The solution changed color from red to violet on the first drop of TEA. The solution was left to stand overnight, during which time it changed color to dark blue and produced a blue precipitate. The entire reaction mixture was applied to a dry silica column (0.75 × 2 in). The column was eluted with acetone to remove a faint red band and leave a dark blue band at the top. The blue band was eluted with 20 mL of methanol. A 5-mL portion of water was added to the blue solution, and it was set aside to concentrate. The solid, 17 mg, was removed by filtration. Yield 85%.

Results and Discussion

Synthesis and Reactivity

General—The chemistry of the iron complexes of ligands H_3L (L = 1–3) is best summarized by the following equilibria.

$$
\begin{array}{ccccc}
e^- + & [FeH_3L]^{3+} & \rightarrow & [FeH_3L]^{2+} \\
 & \uparrow\downarrow & & \uparrow\downarrow \\
e^- + & [FeH_2L]^{2+} & & [FeH_2L]^{+} \\
 & \uparrow\downarrow & & \uparrow\downarrow \\
e^- + & [FeHL]^{+} & & [FeHL] \\
 & \uparrow\downarrow & & \uparrow\downarrow \\
e^- + & [FeL] & \leftarrow & [FeL]^{-}
\end{array}
$$

Horizontal levels represent redox equilibria with iron(III) on the left and iron(II) on the right, and vertical reactions represent acid–base equilibria with the most acidic species at the top. For each of the three ligands studied, $[FeL]^-$ is the most reducing species and has not been isolated to date; but its oxidized product, FeL, is observed. In addition, $[FeH_3L]^{3+}$ is the most oxidizing species for all ligands and is observed for L = 1 and 2 but not for 3. For $H_3(3)$, it is possible (in air) to interconvert between iron(II) and iron(III) by adding acid or base to solutions of any complex of iron and the ligand. All reactions were performed in air, and products were characterized by EA(CHN); IR; UV–vis; MS; CV; Mössbauer; and in three cases, by structural determination. Many products can be produced by more than one method, and in those cases, if the IR and UV–vis spectra of these species were the same, then the products were deemed identical. In the important case of the conversion of Fe(3) to $[FeH_3(3)]^{2+}$ in acid, the product was examined by Mössbauer and ESI-MS, as well, to demonstrate the presence of iron(II). Discussion of this reaction is given at the end of the Synthesis discussion section.

Synthesis of the Cations $[FeH_3(1–3)]^{3+,2+}$—Reaction of iron(II) or iron(III) salts in air with a methanol solution of the ligands, $H_3(1)$–$H_3(3)$, generated in situ by reaction of tren and the appropriate imidazole carboxaldehyde, affords $[FeH_3(1–3)^{2+/3+}]X_{(2\text{ or }3)}$ ($X = ClO_4^-$ or BPh_4^-) in good yields.

$$
\begin{array}{l}
\text{Tren} + \text{imidazole carboxaldehyde} \rightarrow H_3L \xrightarrow{Fe^{2+}\text{ or }Fe^{3+}} \xrightarrow{X^-} \\
[FeH_3L]X_{2\text{or}3}\ \ L = 1-3,\ X = ClO_4^-\text{ or }BPh_4^-
\end{array}
$$

The three ligands show markedly different preferences for iron in either the 2+ or 3+ oxidation state. From the synthetic observations described below, the ease of reduction of iron(III) to iron(II) for the complexes of these ligands is $H_3(3) > H_3(2) > H_3(1)$.

Reaction of $H_3(1)$ with iron(III) chloride followed by addition of sodium perchlorate yields purple $[FeH_3(1)](ClO_4)_3$. Purple methanol solutions of $[FeH_3(1)](ClO_4)_3$ are stable for weeks, as judged by no observable loss of color. The reaction of $H_3(1)$ with iron(II) perchlorate gives blue-green and orange precipitates that were not identified; however, the color of the solids is consistent with a mixture of both iron(III) neutral (blue-green) and iron(II) cationic (orange) products. Although pure $[FeH_3(1)](ClO_4)_2$ was not isolated from the reaction of iron(II) with $H_3(1)$, an iron(II) complex of $H_3(1)$ can be prepared by reduction of $[FeH_3(1)](ClO_4)_3$ with sodium thiosulfate to give orange $[FeH_3(1)]S_4O_6$.

Reaction of $H_3(2)$ with iron(III)chloride (followed by addition of sodium perchlorate) or with iron(II) perchlorate yields purple-red $[FeH_3(2)](ClO_4)_3$ or orange $[FeH_3(2)](ClO_4)_2$, respectively. $[FeH_3(2)](ClO_4)_3$ is isolated from the iron(III) chloride reaction due to its low solubility. However, if it is kept in solution for ~2 days, the color of the solution changes to orange, and very small amounts of an orange complex can be isolated by filtration. This product has the same IR and UV–vis spectral characteristics as $[FeH_3(2)](ClO_4)_2$, produced by direct

reaction of $H_3(2)$ (generated in situ) with iron(II) perchlorate, and is therefore identified. However, given the trace amounts of this species which can be isolated under these conditions, this reaction is not synthetically useful.

With $H_3(3)$, the red iron(II) complex, $[FeH_3(3)]X_2$, is formed from reaction with either an iron (II) or iron(III) starting material. Although uncommon, the isolation of an iron(II) N_6 complex from the reaction of an iron(III) salt with nitrogenous ligands has also been observed with terpyridyl[33] and ethylenediamine[34] and, most recently, with another closely related tripodal tren imidazole ligand.[35] Discussion of the relative sensitivity of the iron(III) complexes to reduction and the probable reducing agent is given in the Ligand Field Effects section at the end of the Discussion. In the reaction of iron(III) chloride with $H_3(3)$, there may be an initial iron(III) product that is not isolated because of its rapid reduction to the iron(II) product. When iron(III) chloride is added to a solution of $H_3(3)$ in methanol, a fleeting dark blue color is observed, which is similar to that of Fe(3) in methanol. This color is rapidly replaced by that of the red $[FeH_3(3)]^{2+}$, which is the product isolated from the reaction. The difference between the reactions of $H_3(2)$ and $H_3(3)$ with iron(III) chloride is 3-fold: (1) With $H_3(3)$, no cationic iron(III) complex, $[FeH_3(3)]^{3+}$, is ever isolated. (2) The length of time it takes for iron(III) to reduce to iron(II) is ~1 min for $H_3(3)$ and several days for $H_3(2)$. (3) The yield of reduced product is high for $H_3(3)$ and only trace for $H_3(2)$.

Synthesis of the Iron(III) Neutral Complexes, Fe(1–2), by Deprotonation of $[FeH_3(1–2)]^{3+}$—Reaction of $[FeH_3(1)](ClO_4)_3$ or $[FeH_3(2)](ClO_4)_3$ with aqueous sodium hydroxide in methanol results in the deep blue low-spin iron(III) products, Fe(1) or Fe(2).

$$[FeH_3L]^{3+} + 3OH^- \rightarrow FeL + 3H_2O \quad L = 1 \text{ or } 2$$

The deprotonation of the iron(III) imidazole complexes appears to be a simple acid–base equilibrium. Titration of $[FeH_3(1)](ClO_4)_3$ with standardized sodium hydroxide (Figure 2) yields a single inflection in the mV vs mole ratio plot at ~2.8. Failure to observe individual steps in the titration indicates that under these conditions, the individual ionization constants differ by <4 orders of magnitude (for example, the triprotic citric acid with pK_a's of 3.13, 4.77, and 6.40 exhibits a single inflection, as well, under these same conditions and in water). An average pK_a of ~8.5 can be estimated and is consistent with the increase in acidity of the pyrrolic H's of imidazole coordinated to transition metals.[36] Removal of these protons can also be achieved by column chromatography on alumina in methanol; the product is eluted as a dark blue band. Acidification of Fe(1) with aqueous hydrochloric acid reforms $[FeH_3(1)]^{3+}$, as described in the Experimental Section.

Synthesis of Iron(III) Neutrals, Fe(1–3), by Oxidation of $[FeH_3(1–3)]^{2+}$—The iron (II) complexes, $[FeH_3(1–3)]^{2+}$, can be converted to iron(III) complexes, Fe(1–3) by removal of three protons and an electron. The reaction scheme (shown above) suggests that this could be done by one of two synthetic routes, treatment with base followed by aerial oxidation or oxidation followed by proton removal. Both of these routes yield the desired iron(III) complexes.

$$FeL \xleftarrow{O_2,\ base} [FeH_3L]^{2+} \xrightarrow{PbO_2,\ alumina} FeL$$

Reaction of the iron(II) complexes ($[FeH_3(1)]S_4O_6$, $[FeH_3(2)](ClO_4)_2$, and $[FeH_3(3)]X_2$) with base (either aqueous sodium hydroxide or triethylamine, TEA) results in a color change from orange or red to violet. On standing in air, the violet solutions turn blue, signifying formation of FeL.

The titration of $[FeH_3(3)](BPh_4)_2$ with standardized NaOH is shown in Figure 3. As in the reaction with $[FeH_3(1)](ClO_4)_3$ (Figure 2), there is a single rise in the plot of mV vs mole ratio; however, this is found at 2.08. The third proton may be removed during oxidation of the starting complex to Fe(3), as the following reaction illustrates.

$$4[FeH_3(3)](BPh_4)_2 + 8NaOH + O_2 \rightarrow 4Fe(3) + 8NaBPh_4 + 10H_2O$$

The stability of the imidazole iron(II) complexes to aerial oxidation suggests that a stronger oxidizing agent than dioxygen is needed for their conversion to the Fe(III) complexes. Treatment of orange methanol solutions of $[FeH_3(1)]S_4O_6$ or $[FeH_3(2)](ClO_4)_2$ or red solutions of $[FeH_3(3)]X_2$ with an excess of lead(IV) oxide ($PbO_2 + 4H^+ + 2e^- \rightarrow Pb^{2+} + 2H_2O$; E° = 1.46 V vs NHE) results in a color change to dark green. Chromatography of the green solutions on alumina results in isolation of the iron(III) complexes, Fe(1–3). The initial green solutions may be the partially deprotonated iron(III) complexes, $[FeH_2L]^{2+}$ or $[FeHL]^+$ or both, which would be expected to form on oxidation, since lead(IV) oxide requires a proton to function as an oxidizing agent. In the absence of added acid, the triprotic iron complex is a logical proton source for the reaction. Consistent with this is the observation that lead(IV) oxide has no effect on the color of solutions of $[Fe(4)]^{2+}$ or $[Fe(5)]^{2+}$,[37] both of which lack ionizable protons. The Fe(III)/Fe(II) reduction potentials of $[Fe(4)](PF_6)_2$[27] and $[Fe(5)](PF_6)_2$[38] are 0.91 and 1.16 V vs NHE, respectively, and that of $[FeH_2(3)]^{2+}$ (this work, 0.299 V vs Ag/Ag^+) is ~1.1 V vs NHE. Thus lead(IV) oxide is a sufficiently strong oxidant (1.46 V) that it should be able to oxidize $[FeH_2(3)]^{2+}$, $[Fe(4)]^{2+}$, and $[Fe(5)]^{2+}$ to their iron(III) products; however, it only results in oxidation for the species with ionizable protons and fails to oxidize those which lack this feature. Removal of the remaining protons from the iron complex in the green solution is achieved on alumina, as described above for $[FeH_3(1–2)]^{3+}$. It is significant to note that treatment with alumina alone does not result in oxidation of the iron(II) protonated complexes, $[FeH_3(1)]^{2+}$, $[FeH_3(2)]^{2+}$ or $[FeH_3(3)]^{2+}$. This reflects the lower acidity of $[FeH_3L]^{2+}$ relative to $[FeH_3L]^{3+}$. The former is only partly deprotonated by the weakly basic alumina, whereas the latter is completely deprotonated. Thus lead(IV) oxide serves to oxidize iron(II) to iron(III) with concurrent partial proton loss from the ligand. Subsequent treatment of the iron(III) complexes with alumina completes the deprotonation and results in production of Fe(1–3).

Reduction of Fe(3) to $[FeH_3(3)]^{2+}$ in Acid—Spontaneous reduction of iron(III) to iron (II) via the presumed intermediate, $[FeH_3(3)]^{3+}$ (as yet unobserved), was found for the reaction of $H_3(3)$ with $FeCl_3$. Following the reaction scheme suggested at the beginning of this discussion, protonation of Fe(3), leading to $[FeH_3(3)]^{3+}$, could likewise be expected to produce $[FeH_3(3)]^{2+}$.

$$Fe(3) + 3H^+ + e^- \xrightarrow{X^-} [FeH_3(3)]X_2X^- = ClO_4^- \text{ or } BPh_4^-$$

Treatment of a blue methanol solution of Fe(3) with 3 equiv of aqueous hydrochloric acid gives a green solution from which the iron(II) complexes can be isolated. Addition of a methanol solution of $NaBPh_4$ results in the immediate precipitation of red $[FeH_3(3)](BPh_4)_2$. Alternately, addition of sodium perchlorate followed by concentration and chromatography yields the red $[FeH_3(3)](ClO_4)_2$. The use of sodium tetraphenylborate as a precipitating agent greatly facilitates the isolation of the iron(II) complex due to its low solubility in methanol.

Since the conversion of Fe(3) to $FeH_3(3)^{2+}$ in acid is a somewhat unexpected outcome, the product of this reaction (Experimental Section, $[FeH_3(3)](BPh_4)_2$, Method b.) was analyzed by several methods, and the results were compared to the analogous results of the product of the direct reaction of iron(II) and $H_3(3)$, generated in situ (Experimental Section, $[FeH_3(3)]$

($BPh_4)_2$, Method a.). The elemental analysis supports that both products are formulated as $[FeH_3(3)](BPh_4)_2$. In addition, the IR, UV–vis, and ESI-MS spectra of these products were obtained and found to be identical. Mössbauer spectra at both room temperature and liquid nitrogen were obtained, as well. At 77 K, both products are essentially LS iron(II), and at room temperature, both products exhibit two sets of peaks with the same values of isomer shifts (method a: 0.38 LS, 1.13 HS; method b: 0.42 LS, 1.14 HS) corresponding to LS and HS iron (II). The LS composition of the two products differs, with that produced from Fe(3) being richer in the LS component (83%) than that produced from direct reaction of iron(II) and $H_3(3)$ (44%). The difference in spin composition and the nature of the reducing agent are discussed in the Ligand Field Effects section at the end of the discussion. The conclusion based on comparison of EA, IR, UV, ESI-MS, and Mössbauer data is that the products of the reactions of iron(II) chloride with $H_3(3)$, generated in situ, (method a) and Fe(3) with acid (method b), followed by treatment with tetraphenylborate, are both $[FeH_3(3)](BPh_4)_2$.

Characterization

Mass Spectroscopy—Mass spectroscopic characterization of the complexes was accomplished by electrospray ionization MS, and the observed *m*/*e* ions are given in Table 2. In all cases in the positive ion mode, an ion corresponding to the desired species was observed as the base peak with little or no other identifiable fragmentation. For some of the perchlorate salts, there is a peak corresponding to the ion plus perchlorate.

UV–Visible Spectroscopy—The UV–visible bands of the various complexes are given in Table 2. The iron(III) neutral complexes, Fe(1–3), are deep blue in methanol or acetonitrile, and the corresponding cationic complexes of iron(III), $[FeH_3(1–2)]^{3+}$ are purple or red-purple. The cationic iron(II) complexes are bright red ($[FeH_3(3)]^{2+}$) or orange ($[FeH_3(1)]^{2+}$ or $[FeH_3(2)^{2+}]$) in the solid state and in solution. In the solid state, the orange iron(II) complexes turn red at liquid N_2 temperature, concomitant with changes in spin-state populations of the ^1A and ^5T states as determined by Mössbauer spectroscopy, presented later in the discussion. This thermochromic behavior (red-LS at low temperature and yellow-orange-HS at high temperature) is characteristic of iron(II) N_6 spin-crossover systems.[39]

IR Spectroscopy—The most useful bands in the IR spectra of these complexes are the imine absorption band(s), given in Table 2, and those attributed to the polyatomic anions, perchlorate, tetraphenylborate, and tetrathionate, of the cationic complexes. The skeletal vibrations for each ligand vary only slightly with the oxidation state of iron and the different levels of protonation. Within these series of complexes, the position of the imine absorption band(s) correlates with the charge of the complex. For each complex, one or two bands are observed between 1640 and 1570 cm^{-1}. The cationic complexes exhibit a more intense absorption above 1600 cm^{-1}, whereas the dominant imine absorption in neutral complexes occurs below 1600 cm^{-1}. It has been previously reported for the 4-imidazolecarboxaldehyde adduct of $[FeH_3(2)](ClO_4)_3$ that the position of the imine absorption is sensitive to the spin state of iron.[25]

Cyclic Voltammetry—The $E_{1/2}$ values for the complexes are given in Table 2 referenced to Ag/Ag^+. The potential of $Fe(phen)_3^{2+}$ under these same conditions was measured at 763 mV, which compares favorably to a literature report using the same reference electrode.[40] The redox processes are reversible one-electron changes based on the difference between E_p cathodic and E_p anodic of 60 mV. The general stabilization of the iron(II) complexes with the imidazole ligands and the stabilization of the iron(III) forms with the fully deprotonated ligands is pronounced. Although the stabilization of iron(II) with nitrogenous donors is often explained on the basis of the low-spin nature of these complexes, additional factors may be at play in the case of $[FeH_3(2)](ClO_4)_2$, which is pure high-spin at room temperature but stable to oxidation in air.

The average difference between the $E_{1/2}$ values of $[FeH_3L]^{3+}$ and FeL for L = 1–3 is 983 mV, an average of 327 mV/proton, which is in approximate agreement with work described for ruthenium and osmium imidazole complexes, 300 mV/proton,[20] and with the value of 345 mV/proton observed for iron imidazole complexes.[21] However, this 1-V window differs slightly with each of the three ligands, the relative ease of reduction being $FeH_3(3)^{3+}$ > $FeH_3(2)^{3+}$ > $FeH_3(1)^{3+}$, the same order that was observed synthetically. The variation of reduction potential with protonation of these complexes suggests that deprotonation of the cationic iron(II) complex facilitates oxidation to iron(III) in air and that acidification of the neutral iron(III) complexes destabilizes the iron(III) state relative to the Fe(II) state. All of the FeL^{-}species are too reducing in air to be observed. The oxidizing species, $FeH_3(1–2)^{3+}$, are isolated, even though they are unstable relative to the iron(II) complexes. However, $FeH_3(3)^{3+}$, which is the most oxidizing, is not observed synthetically.

Mössbauer—The spin state of the iron atom in these complexes was determined by Mössbauer spectroscopy at liquid nitrogen and room temperature. The values of quadrupole splitting (QS) and isomer shift (IS) are given in Table 2.

Iron(III) Neutrals—These complexes, Fe(1–3), are low-spin with large quadrupole splitings, 1.72–2.93 mm/s, and isomer shifts near 0. The stabilization of the low-spin state is expected with iron(III) bound to an N_6 donor set of an anionic ligand.

Iron(III) Cations—Protonation of the imidazole nitrogen decreases the strength of the ligand, which results in stabilization of the high-spin state. At room temperature, $[FeH_3(1)](ClO_4)_3$ exhibits a single peak indicative of a high-spin assignment. $[FeH_3(2)](ClO_4)_3$ exhibits two pairs of peaks at room temperature with QSs of 1.16 (20.5%) and 1.79 (79.5%) mm/s which are assigned as high-spin and low-spin, respectively. On cooling with liquid N_2, the pair with the larger QS grows in intensity, while the inner pair disappears. These observations are consistent with a spin equilibrium between the ^{2}T and ^{6}A states. A spin equilibrium was also observed for the closely related 4-imidazole carboxaldehyde adduct of $[FeH_3(2)](ClO_4)_3$, which has been characterized by variable temperature magnetic susceptibility as being involved in a two-step spin equilibrium.[25] At room temperature, ~75% of the iron is high-spin, and at 77 K, the entire sample is low-spin.

Iron(II) Cations—All of the iron(II) cation complexes, $[FeH_3(1)]S_4O_6$, $[FeH_3(2)](ClO_4)_2$, $[FeH_3(3)](ClO_4)_2$, and $[FeH_3(3)](BPh_4)_2$, are characterized as spin-crossover complexes with an equilibrium between the ^{1}A and ^{5}T states. The difference among the complexes is simply the position of the equilibrium at a given temperature. All of the complexes are predominantly or exclusively high-spin at room temperature and predominantly or exclusively low-spin at liquid nitrogen temperature. Figure 4 shows the Mössbauer spectrum of $[FeH_3(2)](ClO_4)_2$ at 295 and 77 K which illustrates this temperature variation.

The orange complexes, $[FeH_3(1)]S_4O_6$ and $[FeH_3(2)](ClO_4)_2$, darken to red at liquid N_2 temperature, as mentioned earlier, due to thermochromic properties of iron(II) SC complexes.[39] $[FeH_3(3)](ClO_4)_2$ and $[FeH_3(3)](BPh_4)_2$ are both red at room temperature and contain a greater population of the ^{1}A (LS) state than the orange complexes. At room temperature the dominant signal in each complex has a set of peaks featuring both a high QS (>1.5 mm/s) and high IS (>1.1 mm/s), which is assigned to HS iron(II) and, in all but one case, an inner set of peaks of low QS assigned to low-spin iron(II). At liquid N_2 temperature, the intensity of the inner set of peaks increases greatly at the expense of the outer set of peaks, consistent with a spin equilibrium.

Molecular Structures—The structures of $Fe(2)\cdot 3H_2O$, $Fe(3)\cdot 4.5H_2O$, and $[FeH_3(3)](ClO_4)_2\cdot H_2O$ obtained at 100 K bear strong similarities. Although the ligands are potentially

heptadentate, the central iron atom in all three complexes is bound to six N atoms in a distorted octahedron with the three imine N atoms facial and the three imidazole N atoms facial. The distance between the Fe atom and the apical 3° amine N of the ligand is outside of bonding range, varying between 3.14 and 3.44 Å in the three structures. A flattened geometry is observed around N1, which is approximately trigonal planar, with C–N1–C bond angles varying between 117.5° and 120.6°. The geometry about the apical N for complexes of similar ligands derived from tren has been related to coordination number.[41] For the structures reported here and for similar complexes, trigonal planar geometry about the apical N atom has been observed for six coordinate complexes. For seven-coordinate Mn(II),[42] Co(II),[42] and Fe(II)[41] and for a pseudo-seven-coordinate Fe(II) complex[41] of similar tripodal ligands, the geometry around the apical N was found to be pyramidal with the N atom pulled closer to the central Fe atom. Selected bond distances for all of the complexes investigated in this work are found in Table 3.

Fe(2)·3H_2O and Fe(3)·4.5H_2O—The structures of the neutral low-spin iron(III) complexes Fe(2)·3H_2O (Figure 5) and Fe(3)·4.5H_2O (Figure 6) are similar to that of the analogous complex Fe(1)·CH_2Cl_2·2H_2O reported earlier,[23] with all Fe–N bond distances in the three complexes <2.0 Å, as expected for low-spin iron(III).

The bonds between Fe and the imidazolate N atoms are shorter than those observed between Fe and the imine N atoms of the Schiff base linkages, reflecting a stronger interaction between the iron and the basic imidazolate rings. Fe(2)·3H_2O possesses a C_3 axis passing through the Fe atom and the apical N of the tripodal ligand, giving three equivalent Fe–imidazolate N distances of 1.938 Å and three equivalent Fe–imine N distances of 1.988 Å. For Fe(3) ·4.5H_2O, two independent molecules were found in the unit cell with average Fe–imidazolate N distances of 1.933 and 1.936 Å and average Fe–imine N bond distances of 1.993 and 1.990 Å for the two sites, respectively. Bite angles for the three Fe(III) neutral low-spin complexes are also comparable, between 80.7 and 81. 6° for Fe(2)·3H_2O, Fe(3)·4.5H_2O, and Fe(1) ·CH_2Cl_2·2H_2O.

The 293 K structure of the 1:1 adduct of [FeH_3(2)](ClO_4)$_3$ with 4-imidazole carboxaldehyde is spin-crossover, contains two iron sites, and is largely high-spin at room temperature.[25] Average Fe–N distances of two sites are 2.11 and 2.08 Å, which are significantly longer than the distances found in the neutral complex, Fe(2), reported here. Thus, protonation of the imidazoles increases the Fe–N bond distances. This change is consistent with the high-spin characterization of the cation and the low-spin characterization of the neutral species. Longer Fe–imidazole N-bond distances than those observed in the neutral complexes are also consistent with weaker binding by the neutral imidazole ligands than by imidazolate. Bite angles for the two iron sites in the protonated complex are compressed relative to the neutral species, varying between 74.8 and 78.0°.

The structure of an adduct of Fe(3) and Mn(hfa)$_2$ has also been reported as a low-spin Fe(III)–high-spin Mn(II) polymer.[24] An Fe–imidazolate N distance of 1.924 Å in this species and an Fe–imine N distance of 1.983 is comparable to the Fe–N distances found in the neutral low-spin Fe(III) complexes, Fe(1)·CH_2Cl_2·2H_2O, Fe(2)·3H_2O, and Fe(3)·4.5H_2O. Evidently, formation of an adduct with a neutral Lewis acid such as Mn(hfa)$_2$ has no significant effect on Fe–N distances or spin state, whereas protonation and creation of the cation results in a change from low- to high-spin and longer Fe–N bond distances.

FeH_3(3)(ClO_4)$_2$·H_2O—The structure of [FeH_3(3)](ClO_4)$_2$·H_2O is shown in Figure 7.

At 100 K, the Fe(II) complex is essentially low-spin, and its structure is close to that of the low-spin neutral Fe(III) complex Fe(3)·4.5H_2O. An average Fe–imidazole N distance of 1.964

Å and an average Fe–imine N distance of 1.980 are similar to those observed for the neutral low-spin Fe(III) species of the same ligand and consistent with average Fe–pyridine N and Fe–imine N distances of 1.95 and 1.98 Å, respectively, reported for a similar Fe(II) low-spin complex, [Fe(5)]$(BF_4)_2$.[28] In contrast, the average Fe–N distance of 2.22 Å found for high-spin [Fe(4)]$(PF_6)_2$[27] is significantly longer than that found for either [FeH_3(3)]$(ClO_4)_2$ or [Fe(5)]$(PF_6)_2$. The bite angles in this complex vary from 80.7 to 80.9°, also similar to that found in the low-spin neutral iron(III) complex of this ligand.

Ligand Field Effects and Implications for Solution Chemistry—The cationic iron (II) complexes of H_3(1–3) (this work), (4),[37] and (5),[38] $[Fe(L)]^{2+}$, have all been prepared and characterized. By Mössbauer spectroscopy, $[Fe(5)]^{2+}$ is pure LS, whereas the red $[FeH_3(3)]^{2+}$ and $[Fe(4)]^{2+}$ are ~32% LS at room temperature. The yellow-orange $[FeH_3(1)]^{2+}$ (23%) and $[FeH_3(2)]^{2+}$ (0%) complexes have even lower LS iron(II) components at room temperature. On the basis of this observation, the approximate order of ligand field strength of these ligands is as follows:

$$(5) > H_3(3) \sim (4) > H_3(1) > H_3(2)$$

It may be that the distinction between [FeH_3(1)] and $[FeH_3(2)]^{2+}$ is in part due to differences attributed to the counterion, tetrathionate for the former and perchlorate for the latter. However it is clear that both H_3(1) and H_3(2) provide a lower ligand field (smaller percent composition of ^{1}A state) than the others on the basis of Mössbauer data, and this is consistent with the fact that these complexes are yellow-orange, as opposed to red.

With iron(III) and the neutral ligands, only [FeH_3(1)]$(ClO_4)_3$ (0% LS) and [FeH_3(2)]$(ClO_4)_3$ (80% LS) have been prepared, and on the basis of Mössbauer data, the order of ligand field strength is H_3(2) > H_3(1). The iron(III) neutral complexes, Fe(1), Fe(2), and Fe(3), are all pure LS, so no ordering of the ligand field effects of the anions, L^{3-}, can be done. The effect of deprotonation of the imidazole to imidazolate can be observed in comparing the spin states of [FeH_3(1)]$(ClO_4)_3$ with Fe(1) and [FeH_3(2)]$(ClO_4)_3$ with Fe(2). The result is that the ligand field strength of the imidazolate species is greater than the neutral imidazoles, $(1)^{3-} > H_3(1)$ and $(2)^{3-} > H_3(2)$, as would be predicted on the basis of charge. Although this same measurement cannot be made for H_3(3) because its iron(III) complex is not observed, it is almost certain that the same trend is followed and the field of $(3)^{3-}$ is greater than H_3(3). On the basis of the available iron(II) and iron(III) complexes, the approximate ligand field strengths are

$$(5) > H_3(3) \sim (4) > H_3(2) > H_3(1) \text{ and}$$

$$(1)^{3-} > H_3(1), \quad (2)^{3-} > H_3(2), \quad (3)^{3-} > H_3(3)$$

There are two questions regarding these complexes which have not been addressed. These are (1) why is it not possible to isolate $[FeH_3(3)]^{3+}$ (under the conditions employed)? and (2) what is the likely reducing agent in the conversion of the hypothetical $[FeH_3(3)]^{3+}$ to $[FeH_3(3)]^{2+}$ or Fe(3) to $[FeH_3(3)]^{2+}$ in acid? Correlation of the above ranking of ligand field strength with synthetic observations provides some direction on the first question, and the reaction of iron (III) porphyrins with amines provides some clues to both questions.

The failure (to date) to isolate $[FeH_3(3)]^{3+}$ from a reaction of iron(III) and H_3(3) (generated in situ) does not seem that unusual in light of the fact that direct reaction of iron(III) with 4 and 5[37] also results in isolation of the iron(II) complex and not the iron(III) complex. Thus, the spontaneous reduction of iron(III) to iron(II) reported here for H_3(3) is not an anomaly, but part of a larger pattern. The key to predicting which iron(III) cationic complexes can be isolated

([$FeH_3(1)$]$^{3+}$ and [$FeH_3(2)$]$^{3+}$) and which undergo spontaneous reduction ([Fe(5)]$^{3+}$, [$FeH_3(3)$]$^{3+}$, and [Fe(4)]$^{3+}$) may be the LS character of the iron(II) complex. As the LS character of the iron(II) complex increases, its stability relative to the iron(III) complex increases. The considerable back-bonding interaction with the αα′-diimine ligands (–N═C–C═N–) such as those used in this work should contribute to this. Thus, the stabilization of iron (II) over iron(III) in air with these nitrogenous ligands can be attributed at least in part to spin-state effects and those ligands with the larger CFSE stabilize iron(II) over iron(III) to the point that the iron(III) complexes are not observed with all ligands.

In a mechanistic investigation of the reduction of iron(III) porphyrins with amines, it was determined that the bisligated iron(III) porphyrin, Fe(por)L_2^+, species was reduced by amines and that the products were iron(II) bisligated porphyrin, Fe(por)L_2, and imine.[43] It was determined that this reaction likely followed an outer sphere mechanism, that only LS iron(III) was reduced (HS iron(III) failed to reduce under these conditions), and that a primary or secondary aliphatic amine was required for reactivity (>CH–NH– → >C═N– + $2H^+$ + $2e^-$). The spin-state dependency on reactivity is similar to that observed in the present system. That is, solutions of iron(III) and the stronger field ligands (5, $H_3(3)$, and 4) spontaneously reduce to iron(II), and those containing the weaker field ligands ($H_3(1)$ and $H_3(2)$) give an iron(III) complex. This is entirely consistent with the arguments of the previous paragraph. It was mentioned earlier in the synthesis discussion that the [$FeH_3(3)$](BPh_4)$_2$ produced in the reduction of Fe(3) with acid was richer in LS component (83 vs 44%) than was the same species isolated from direct reaction of iron(II) chloride with $H_3(3)$ (generated in situ). In the former reaction, all of the iron is initially present as LS Fe(3), whereas in the latter reaction, all of the iron is initially present as HS ferrous ion. The difference in spin composition could be due to the different initial iron spin states and the reaction conditions employed in the isolation of [$FeH_3(3)$](BPh_4)$_2$.

The identity of the reducing agent in the reactions of iron(III) with $H_3(3)$ (generated in situ) or Fe(3) with acid to give [$FeH_3(3)$]$^{2+}$ is unknown. However, since there is no obvious reducing agent in these reaction mixtures, it is reasonable to consider the ligand as a potential reducing agent. The ligand, $H_3(3)$, is an imine, which is the oxidized form of the amine, so its direct use as a reducing agent is also unlikely. However, hydrolysis or partial hydrolysis of $H_3(3)$ would produce some free tren or at least a ligand with an arm of the tren free, R_2–N–$CH_2CH_2NH_2$. These free amine functionalities should be able to serve as reducing agents, just as described above in the reduction of iron(III) porphyrins. Such cannibalization of the ligand (if it occurs) would reduce the yield of [$FeH_3(3)$]$^{2+}$ in reactions requiring this process. In fact, the percent yield of [$FeH_3(3)$](BPh_4)$_2$ from direct reaction of iron(II) and $H_3(3)$ (method a, 80%) is larger than that of the reaction of Fe(3) with acid (method b, 55%). More detailed mechanistic investigation of this process, including the possible role of tren, will be examined.

Conclusion

A series of iron complexes with three different tripodal imidazole/imidazolate ligands has been prepared and characterized. The structural and electronic effects of deprotonation of the imidazole group on the spin state and oxidation state of the iron were examined. In general, it is observed that the fully protonated ligands stabilize the iron(II) state, and fully deprotonated ligands stabilize the iron(III) state. This was observed synthetically and verified by $E_{1/2}$ measurements. The latter reveal a difference of ~1 V between the reduction potential of the fully protonated ligands and the fully deprotonated ligands, which corresponds to 327 mV/proton change in reduction potential upon deprotonation. The order of ligands in terms of ease of reduction of the iron(III) complexes is $H_3(3)$ > $H_3(2)$ > $H_3(1)$. With $H_3(3)$, it is not possible to isolate the iron(III) complex, even beginning with an iron(III) salt; however, it is possible to isolate fully protonated iron(III) complexes with $H_3(1)$ and $H_3(2)$. The dramatic dependence

of $E_{1/2}$ on protonation level explains why all iron(II) protonated complexes, $[FeH_3L]^{2+}$, produce the iron(III) neutral complexes, FeL, on treatment with base in air. Protonation of the iron(III) complex, Fe(3), gives the iron(II) complex, $[FeH_3(3)]^{2+}$. The interconversion of $[FeH_3(3)]^{2+}$ and Fe(3) is an interesting and structurally characterized example of an acid–base-promoted redox reaction. Mössbauer results indicate that the ligand field strength of these and related ligands is $5 > 4 \sim H_3(3) > H_3(2) > H_3(1)$ on the basis of overlapping series of iron(II) and iron(III) complexes. Deprotonation of $H_3(2)$ and $H_3(1)$ increases their ligand field strength.

Supplementary Material

Refer to Web version on PubMed Central for supplementary material.

Acknowledgements

The support provided by NIH Grant GM-38401 to W.R.S. is gratefully acknowledged. Some of the mass spectral data was obtained at the University of Massachusetts Mass Spectrometry facility, which is supported in part by the National Science Foundation.

References

1. O'Brien P, Sweigart DA. Inorg Chem 1985;24:1405–1409.
2. Traylor TG. Acc Chem Res 1981;14:102–109.
3. Slattery AJ, Blaho JK, Lehnes J, Goldsby KA. Coord Chem Rev 1998;174:391–416.
4. Takeuchi KJ, Samuels GJ, Gersten SW, Meyer TJ. Inorg Chem 1983:1407–1409.
5. Dobson JC, Meyer TJ. Inorg Chem 1988;27:3283–3291.
6. Llobet A, Doppelt P, Meyer TJ. Inorg Chem 1988;27:514–520.
7. Hage R, Krijnen B, Warnaar JB, Hartl F, Stufkens DJ, Snoeck TL. Inorg Chem 1995;34:4973–4978.
8. Wong K, Che C, Li C, Chui W, Zhou Z, Mak TCW. J Chem Soc, Chem Commun 1992:754–756.
9. Bernhard P, Anson FC. Inorg Chem 1989;28:2–3274.
10. Caudle MT, Pecoraro VL. Inorg Chem 2000;39:5831–5837. [PubMed: 11151386]
11. Hays AA, Vassiliev IR, Golbeck JH, Debus RJ. Biochemistry 1998;37:11352–11365. [PubMed: 9698383]
12. Aedelroth P, Paddock ML, Tehrani A, Beatty JT, Feher G, Okamura MY. Biochemistry 2001;40:14538–14546. [PubMed: 11724567]
13. Buchanan BE, Wang R, Vos JG, Hage R, Haasnoot JG, Reedijk J. Inorg Chem 1990;29:3263–3265.
14. Hage R, Prins R, Haasnoot JG, Reedijk J, Vos JG. J Chem Soc, Dalton Trans 1987:1389–1395.
15. Sullivan BP, Salmon DJ, Meyer TJ, Peedin J. Inorg Chem 1979;18:3369–3374.
16. Mohanty JG, Chakravorty A. Inorg Chem 1976;15:2912–2916.
17. Singh AN, Singh RP, Mohanty JG, Chakravorty A. Inorg Chem 1977;16:2597–2601.
18. Mohanty JG, Chakravorty A. Inorg Chem 1977;16:1561–1563.
19. Bond AM, Haga M. Inorg Chem 1986;25:4507–4514.
20. Haga M, Ano T, Kano K, Yamabe S. Inorg Chem 1991;30:3843–3849.
21. Carina RF, Verzegnazzi L, Bernardinelli G, Williams AF. Chem Commun 1998:2681–2682.
22. Burnett MG, McKee V, Nelson SM. J Chem Soc, Chem Commun 1980:599–600.
23. Brewer CT, Brewer G, Shang M, Scheidt WR, Muller I. Inorg Chim Acta 1998;278:197–201.
24. Lambert F, Renault JP, Policar C, Morgenstern-Badarau I, Cesario M. J Chem Soc, Chem Commun 2000:35–36.
25. Sunatsuki Y, Sakata M, Matsuzaki S, Matsumoto N, Kojima M. Chem Lett 2001:1254–1255.
26. Sunatsuki Y, Ikuta Y, Matsumoto N, Ohta H, Kojima M, Iijima S, Hayami S, Maeda Y, Kaizaki S, Dahan F, Tuchauges JP. Angew Chem, Int Ed 2003;42:1614–18.
27. Yang S, Tong Y, Zhu H, Cao H, Chen X, Ji L. Polyhedron 2001;20:223–229.
28. Mealli C, Lingafelter EC. J Chem Soc, Chem Commun 1970:885.

29. Lippard, SJ.; Berg, JM. Principles of Bioinorganic Chemistry. University Science Books; Mill Valley, CA: 1994.
30. Yachandra VK, DeRose VJ, Latimer MJ, Mukerji I, Sauer K, Klein MP. Science 1993;260:675. [PubMed: 8480177]
31. Sheldrick GM. Acta Crystallogr 1990;A46:467–470.
32. Sheldrick, G. M. SHELXL-97: FORTRAN program for crystal structure refinement, {copyright} 1997, Göttingen University.
33. Reiff WM, Baker WA, Erickson NE. J Am Chem Soc 1968;90:4794–4800.
34. Fowles GWA, McGregor WR. J Chem Soc 1958:136–140.
35. (a) Ikuta Y, Ooidemizu M, Yamahata Y, Yamada M, Osa S, Matsumoto N, Iijima S, Sunatsuki Y, Kojima M, Dahan F, Tuchauges JP. Inorg Chem 2003;42:7001–7017. [PubMed: 14577766] (b) Yamada M, Ooidemizu M, Ikuta Y, Osa S, Matsumoto N, Iijima S, Kojima M, Dahan F, Tuchagues JP. Inorg Chem 2003;42:8406–8416. [PubMed: 14658894]
36. Sundberg RJ, Martin RB. Chem Rev 1974;74:471–517.
37. Brewer CT, Brewer G, Luckett C, May L, Beatty AM, Scheidt WR. Inorg Chim Acta. 2004in press
38. Hoselton MA, Wilson LJ, Drago RS. J Am Chem Soc 1975;97:1722–1729.
39. Sugiyarto KH, McHale WA, Craig DC, Rae AD, Scudder ML, Goodwin HA. Dalton Trans 2003:2443–2448.
40. Addison AW, Burman S, Wahlgren CG, Rajan OA, Rowe TM, Sinn E. J Chem Soc, Dalton Trans 1987:2621–2630.
41. Morgenstern-Badarau I, Lambert F, Renault JP, Cesario M, Marechal J, Maseras F. Inorg Chim Acta 2000;297:338–350.
42. Gou S, You X, Yu K, Lu J. Inorg Chem 1993;32:1883–1886.
43. Castro CE, Jamin M, Yokoyama W, Wade R. J Am Chem Soc 1986;108:4179–4187.

Abbreviations

CSFE
Crystal Field Stabilization Energy

HS
high spin

LS
low spin

NHE
normal hydrogen electrode

PCET
proton-coupled electron transfer

TEA
triethylamine

tren
tris(2-aminoethyl)amine

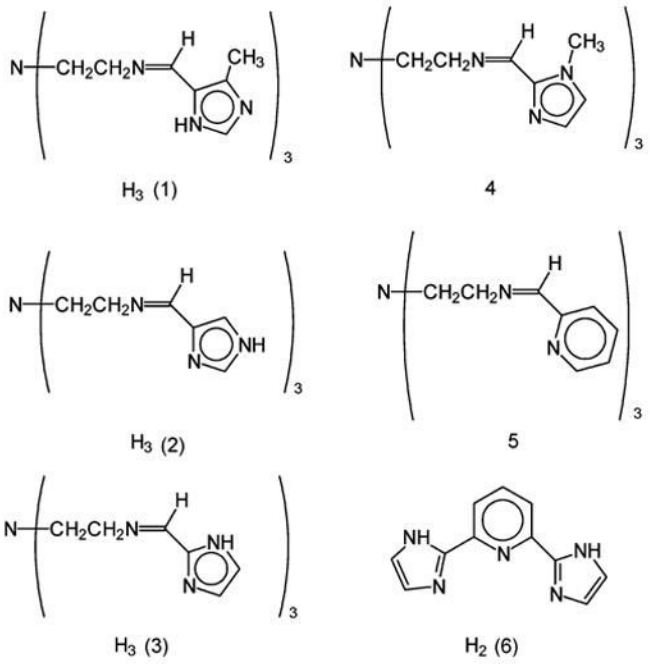

Figure 1.
Line drawings of ligands.

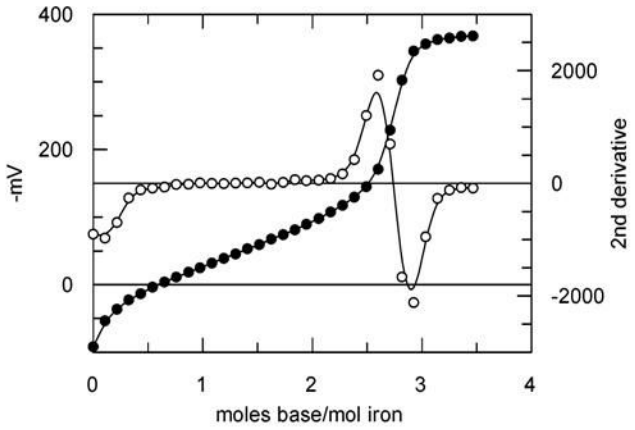

Figure 2.
Titration of $[FeH_3(1)](ClO_4)_3$ with standard NaOH. Darkened circles represent mV and open circles represent the second derivative. Conditions are as described in the Experimental Section.

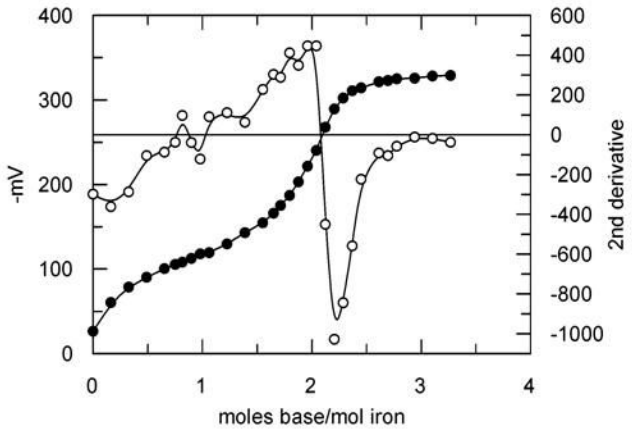

Figure 3.
Titration of $[FeH_3(3)](BPh_4)_2$with standard NaOH. Darkened circles represent mV and open circles represent the second derivative. Conditions are described in the Experimental Section.

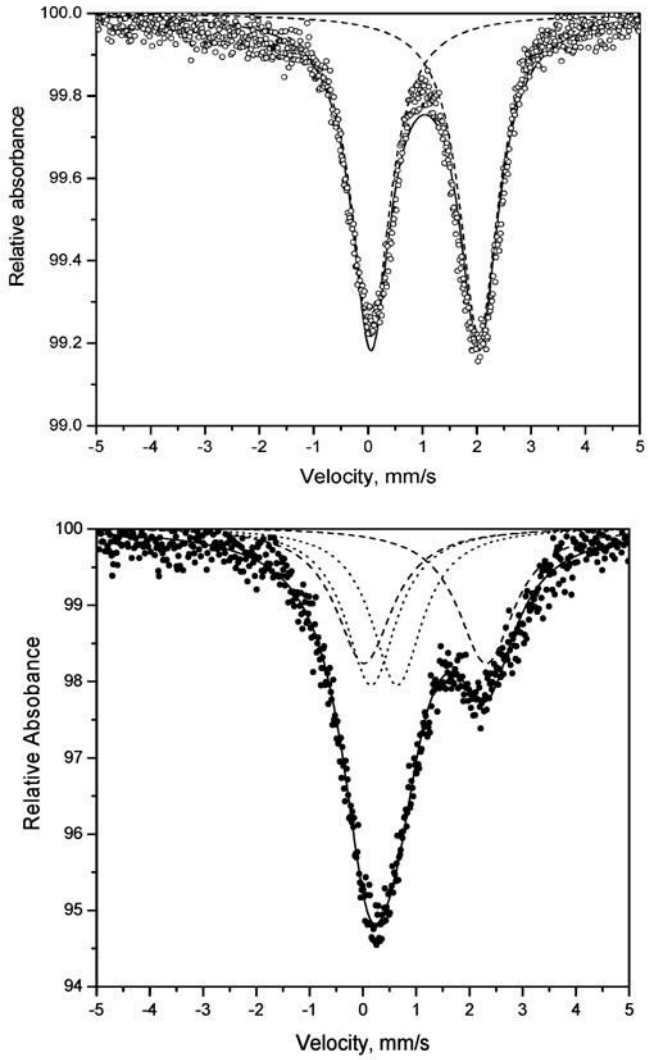

Figure 4.
Mössbauer spectrum of $[FeH_3(2)](ClO_4)_2$ at 295 K (top) and 77 K (bottom).

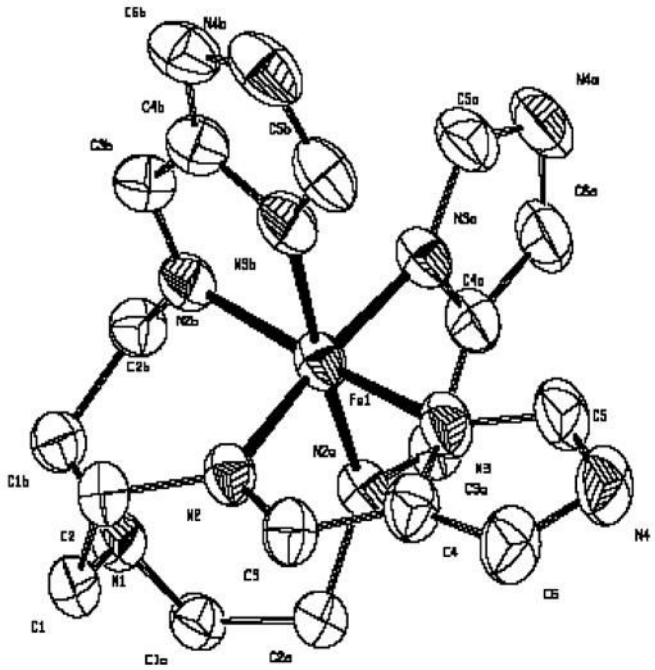

Figure 5.
ORTEP diagram of Fe(2). Atoms are contoured at the 50% probability level, and hydrogen atoms have been omitted for clarity.

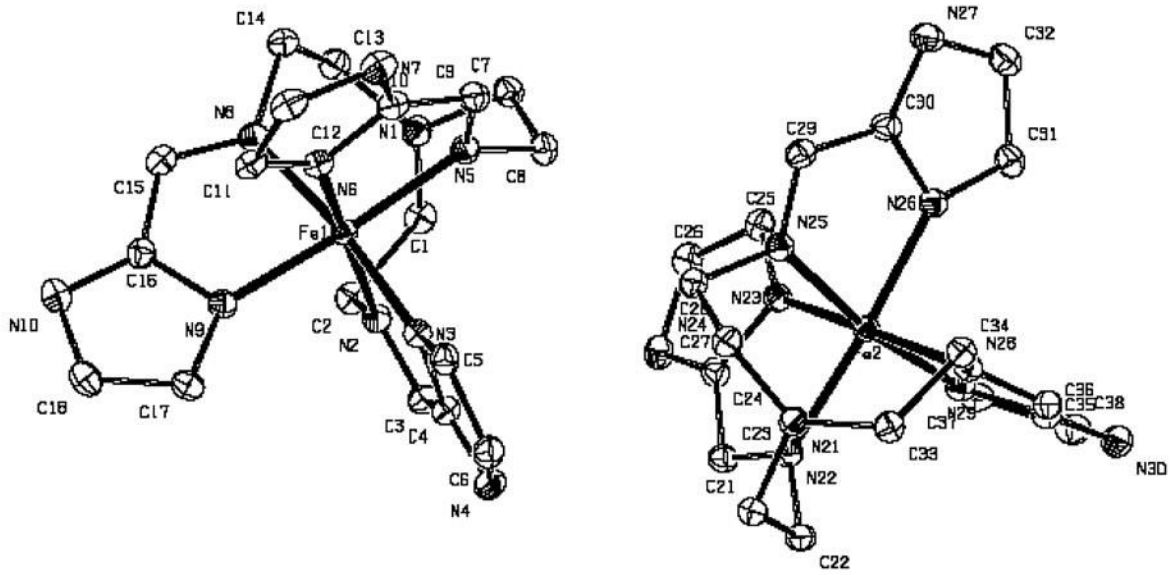

Figure 6.
ORTEP diagram of two independent molecules of Fe(3). Atoms are contoured at the 50% probability level, and hydrogen atoms have been omitted for clarity.

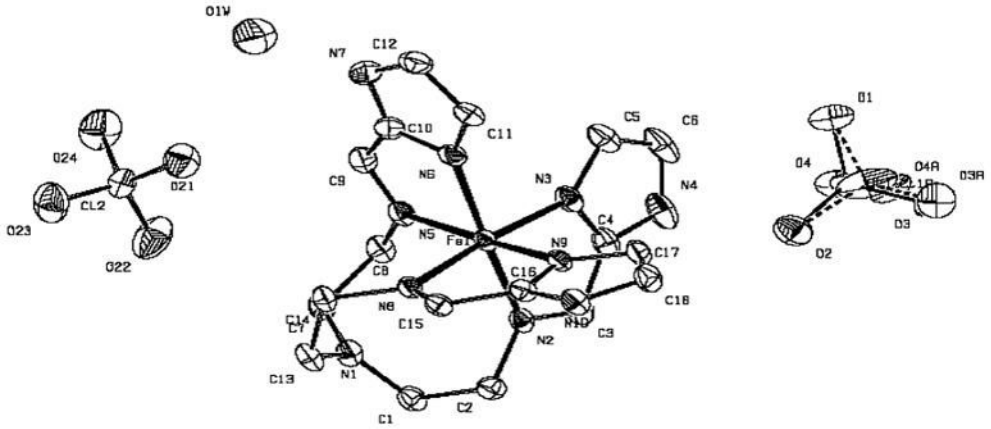

Figure 7.

ORTEP diagram of $[FeH_3(3)](ClO_4)_2 \cdot H_2O$. Atoms are contoured at the 50% probability level, and hydrogen atoms have been omitted for clarity. The ordered and disordered perchlorates are shown.

Table 1

Crystal Data for $Fe(2)\cdot 3H_2O$, $Fe(3)\cdot 4.5H_2O$, and $[FeH_3(3)](ClO_4)_2\cdot H_2O$

	$Fe(2)\cdot 3H_2O$	**$Fe(3)\cdot 4.5H_2O$**	**$[FeH_3(3)](ClO_4)_2\cdot H_2O$**
chem formula	$C_{18}H_{27}FeN_{10}O_3$	$C_{18}H_{30}FeN_{10}O_{4.5}$	$C_{18}H_{26}Cl_2FeN_{10}O_9$
Fw	487.35	514.37	653.24
temp, K	100	100	100
space group	*I*43d	*P*2(1)/*c*	*P*2(1)/*n*
unit cell dimensions	*a* = 20.2707(5) Å	*a* = 20.9986(10) Å	*a* = 9.4848(4) Å
	b = 20.2707(5) Å	*b* = 11.7098(5) Å	*b* = 23.2354(9) Å
	c = 20.2707(5) Å	*c* = 19.9405(9) Å	*c* = 12.2048(5) Å
	α = 90°	α = 90.00°	α = 90°
	β= 90°	*β*= 109.141(1)°	*β*= 111.147(1)°
	γ = 90°	*γ* = 90.00°	*γ* = 90°
Vol	8329.3(4) $Å^3$	4632.1(4) $Å^3$	2508.60(18)) $Å^3$
Z	16	8	4
L	0.71073 Å	0.71073 Å	0.71073 Å
M	0 0.770 mm^{-1}	0.701 mm^{-1}	0.886 mm^{-1}
D_{calcd}	1.555 Mg m^{-3}	1.475 Mg m^{-3}	1.730 Mg m^{-3}
R	0.0363	0.0344	0.0603
R_w	0.0994	0.0860	0.1212

Table 2

Spectral and Electrochemical Values for All Complexes

complex	MS[a]	UV–vis[b]	IR[c]	$E_{1/2}$[d]	Mössbauer[e]			
					T, K	QS	IS	%
			Iron(III) Cations					
$[FeH_3(1)](ClO_4)_3$	477 $(M - H)^+$	268, 533	1632, 1592	0.083	298	0.00	0.29	
$[FeH_3(2)](ClO_4)_3$	434 $(M - 2H)^+$	259, 498	1630	0.170	298	1.16, 1.79	0.30, −0.14	20.5, 79.5
	632 $(M - 2H + 2ClO_4)^-$				77	2.12	−0.12	
			Iron(II) Cations					
$[FeH_3(1)]S_4O_6$	477 $(M - H)^+$	261, 448	1633	0.032	298	2.05	1.14	76.9
			1592			0.00	0.22	23.1
	475 $(M - 3H)^-$				77	2.18	1.19	4.8
						0.41	0.49	95.2
$[FeH_3(2)](ClO_4)_2$	435 $(M - H)^+$	251, 440	1637	0.168	298	1.98	1.18	
	433 $(M - 3H)^-$				77	2.12	1.39	48.6
	535 $(M + ClO_4)^-$ (only trace)					0.59	0.47	51.4
$[FeH_3(3)](ClO_4)_2$	436 (M^+)	280, 489, 524 (sh)	1631	0.306	298	2.14	1.17	68.0
			1578			0.40	0.27	32.0
					77	0.36	0.41	
$[FeH_3(3)](BPh_4)_2$	435 $(M - H)^+$	268, 275, 499[f]	1628	0.299	298	2.08	1.13	55.0
			1579			0.33	0.38	44.3
	319 $(BPh)_4^-$				77	0.49	0.41	
			Iron(III) Neutrals					
Fe(1)	476 $(M + H)^+$	297, 563, 635	1595	−0.900	298	1.72	−0.27	
Fe(2)	434 $(M + H)^+$	290, 562, 617	1596	−0.698	298	2.06	0.14	
Fe(3)	434 $(M + H)^+$	320, 560, 677	1633, 1577	−0.783	298	2.93	0.12	

[a] ESI with methanol.

[b] In methanol.

[c] In KBr.

[d] Relative to Ag/Ag^+ reference electrode in acetonitrile.

[e] All values relative to Fe foil in mm/s. The approximate composition of HS and LS forms is given as a percentage.

[f] In acetonitrile.

Table 3

Selected Intramolecular Distances (Å)[a] and Bond Angles (°)[b] for Fe(1)·CH_2Cl_2·$2H_2O$[c] Fe(2)·$3H_2O$[d] Fe(3)·$4.5H_2O$,[e] and $[FeH_3(3)](ClO_4)_2$·H_2O

	Fe(1)·CH_2Cl_2·$2H_2O$	Fe(2)·$3H_2O$	Fe(3)·$4.5H_2O$	[FeH_3(3)] (ClO_4)$_2$·H_2O
Fe–N3	1.941 (2)	1.9384 (18)	1.9307 (10), 1.9333 (10)	1.958 (2)
Fe–N6	1.936 (2)		1.9368 (10), 1.9423 (10)	1.967 (2)
Fe–N9	1.945 (2)		1.9326 (11), 1.9330 (11)	1.968 (2)
Fe–N2	1.987 (2)	1.9877 (18)	1.9964 (10), 1.9898 (10)	1.974 (2)
Fe–N5	1.979 (2)		1.9885 (10), 1.9911 (10)	1.976 (2)
Fe–N8	1.978 (2)		1.9941 (10), 1.9902 (10)	1.989 (2)
Fe–N1	3.117	3.201	3.137	3.437
N2–Fe–N3	81.11 (7)	80.96 (2)	80.72 (4), 80.97 (4)	80.68 (9)
N5–Fe–N6	81.39 (7)		80.70 (4), 80.95 (4)	80.89 (9)
N8–Fe–N9	81.56 (8)		80.97 (4), 81.10(4)	80.75(8)
N2–Fe–N6	174.38 (7)	173.72(8)	171.87 (4), 172.58(4)	173.99(8)
N3–Fe–N8	175.94 (8)		172.68 (4), 173.10(4)	173.67(9)
N5–Fe–N9	175.58 (8)		170.27 (4), 170.55(4)	171.92(9)

[a] N3, N6, and N9 are imidazole nitrogen atoms; N2, N5, and N8 are imine nitrogen atoms; and N1 is the center nitrogen atom of tren.

[b] Angles are given for the bite angle of the bidentate arm and the trans positions.

[c] Ref 23.

[d] Because of the 3-fold symmetry, there is only one unique imidazole and imine nitrogen atom, N2 and N3, respectively.

[e] Values are given as pairs because there are two iron complexes.